Sustainability in Environment
ISSN 2470-637X (Print) ISSN 2470-6388 (Online)
Vol. 8, No. 1, 2023
www.scholink.org/ojs/index.php/se

Original Paper

Geochemical Speciation and Principal Component Analysis of Toxic Metals in River Ogun Coastal Sediments, Southwestern Nigeria

Olusiji Samuel Ayodele[1], Adedeji Adebukola Adelodun[2*] & David Rasaq Kazeem[2]

[1] Department of Applied Geology, School of Earth and Mineral Sciences, The Federal University of Technology, Akure, Nigeria

[2] Department of Marine Science and Technology, School of Earth and Mineral Sciences, The Federal University of Technology, Akure, Nigeria

[*] Adedeji Adebukola Adelodun, E-mail: osayodele@futa.edu.ng

Received: December 28, 2022 Accepted: January 20, 2023 Online Published: February 1, 2023
doi:10.22158/se.v8n1p33 URL: http://dx.doi.org/10.22158/se.v8n1p33

Abstract

This study investigated the influence and interactions of geochemical fractions of toxic metals in sediments of River Ogun in Nigeria. Fe, Mn, Zn, Pb, Cr, and Co were significantly present across the area, while Cu, Ni, and Cd were negligible. All the metals, except Zn, were found highly above their permissible limits in sediments. The bulk metal concentrations followed the trend: Fe >> Mn > Zn > Pb > Co >> Cu ≈ Cr ≈Ni >> Cd. At p = 0.05, the concentrations (ppm) of Ni, Zn, Co, Mn, Fe, Pb, Cr, Cd, and Cu in the F1 were 1.72–5.84, 13.2–15.0, 1.16–3.41, 56.1–77.2, 198–212, 9.32–14.3, 1.96–3.66, 0.55–1.61, and 0.56–1.98, respectively, while the values were 12.1–13.6, 113–270, 67.8–152, 206–275, 514–637, 131–179, 18.5–27.0, 1.31–1.75, and 6.11–8.11 for the F5, respectively. Overall, Cd and Fe showed the least and highest distributions in the various geochemical forms, respectively. Moreover, the abundance and mobility of Mn, Ni, Fe, Cr, Cd, and Zn correlated significantly in exchangeable and carbonate-bond fractions. Hence, environmental monitoring of the sediments and Pisces should be carried out while remediation of the location is recommended.

Keywords

river ogun, sediments, toxic metals, sequential extraction, correlation

1. Introduction

The astronomical increase in population growth, mechanized farming, and industrialization have resulted in high water demand for industrial and domestic uses in Nigeria (NODS, 2014). Such an increase in industrial activities is often accompanied by environmental pollution. For instance, Isheri, Isasi, and Mawere are communities located around the Ogun River in Southwestern Nigeria. With more than 20 major and 100 minor manufacturing and processing firms, these communities exemplify the rapid industrial growth in recent years. Based on the 2009 census, these communities had a cumulative human population of 165,342, compared to 159,627 and 8,765 reported in 2006 and 1948, respectively (NODS, 2014). However, this population growth has not been accompanied by access to quality water supplies and sanitation (Rahman, 2011).

The Ogun River joined the streams in Isheri, Isasi, and Mawere communities near an abattoir. A similar environmental setup, including raw sewage, industrial effluents, and community wastewater, has been confirmed as a significant source of trace metal deposition (Gathua, 2015). Sediments are a sink for pollutants, reintroducing toxins into the food chain. In aquatic sediments, toxic metals are predominant in the fine-grained fractions (Dithobolong et al., 2021; Olumayede & Ediagbonya, 2018; Helen & Okiemen, 2021). However, some studies have indicated otherwise (Li et al., 2019; Samuel & Olabode, 2021).

The specific surface area of sediments depends on the granulometric parameter and mineral composition (Gafar & Hilmat, 2018). The association of metals with smaller grain-size particles is attributed to co-precipitation and complexation processes (Ho *et al.*, 2010). Most metals occur in a complex form with insoluble inorganic and organic ligands. Thus, toxic metals often absorb onto clays and other fine-grained materials (Ho *et al.*, 2010). The metals adsorb onto negatively charged surfaces of clays, organic matter, iron and manganese oxides, and hydroxides.

Bioavailable metal species are liable and are affected by ecological changes. Thus, geochemical speciation of metals is adopted to identify human susceptibility to these species (Aiyesanmi et al., 2020; Al-mur, 2019; Akinnawo *et al., 2015*; Kotoky *et al.*, 2003; Korfali & Davies, 2004). Sequential extraction provides detailed information about the origin, mode of occurrence, biological and physicochemical availability, mobilization, and transport of toxic metals, although time-consuming. (Tessier et *al.*, 1979). The species are exchangeable, carbonate-bound, reducible, organic-bound, and residual fractions.

Through sequential extraction, Al-Mur (2019) assessed the geochemical speciation of Mn, Fe, Cu, Pb, Zn, Cd, and Ni in the surface sediments of the Jeddah coastal zone of the Red Sea in Saudi Arabia. It was reported that the concentration of toxic metals varies by location. Also, Fe, Mn, Zn, and Pb were abundant in exchangeable fractions, unlike Cd and Ni found in low exchangeable fractions. However, the speciation of Fe, Mn, Cu, Zn, Pb, and Ni in the samples exhibited high-to-medium risks to the aquatic environments. The current study evaluates the geochemical speciation of toxic metals in the coastal sediments from Ogun River in Lagos State, southern western Nigeria, into five operationally defined fractions viz. exchangeable (F1), carbonate-bound (F2), Fe-Mn oxide-bound (F4), organic-bound (F4), and residual (F5) fractions via sequential extraction techniques. This exercise investigates the geochemical affinities and distribution in each fraction and their interactions with the soils of the study area, living organisms, and ecosystems. This extraction technique aims to identify the elemental assemblages in the different geochemical fractions of the metals in Ogun River sediments, enabling the evaluation of their potency and bioavailability toward providing appropriate environmental solutions to the authorities and residents.

1.1 Study Area

Ogun River, running between Ogun and Lagos States, is a prominent river in southwestern Nigeria. The river is located within latitudes 6^o 26’ N longitudes and 4^o 8’ E, covering approximately 23,000 km^2 (**Figure 1**). The study area is a waterway interconnected with major road networks. The location is densely populated with small- and large-scale industries, abattoirs, market stalls, schools, government and private hospitals, and gas stations. The primary occupations of the inhabitants are farming, hunting, and fishing while running abattoirs has been the chief occupation for many years. In addition, sand mining is also prominent along the river channels. The river originates from the Iganran hills at 530 m elevation, and it flows directly southwards over 480 km before discharging into the Lagos lagoon. The major tributaries are the Ofiki and Opeki Rivers. The foliation and the joints on the rocks control the course of the rivers, resulting in a trellis drainage pattern, particularly at the north of the study area.

The lithosphere is predominantly organic-hydromorphic and ferrallitic soils. The basement rocks that underline the basin line are titled towards the south Atlantic and have been faulted into horsts and graben structures (Ayodele et al., 2019; Omatsola & Adegoke, 1981).

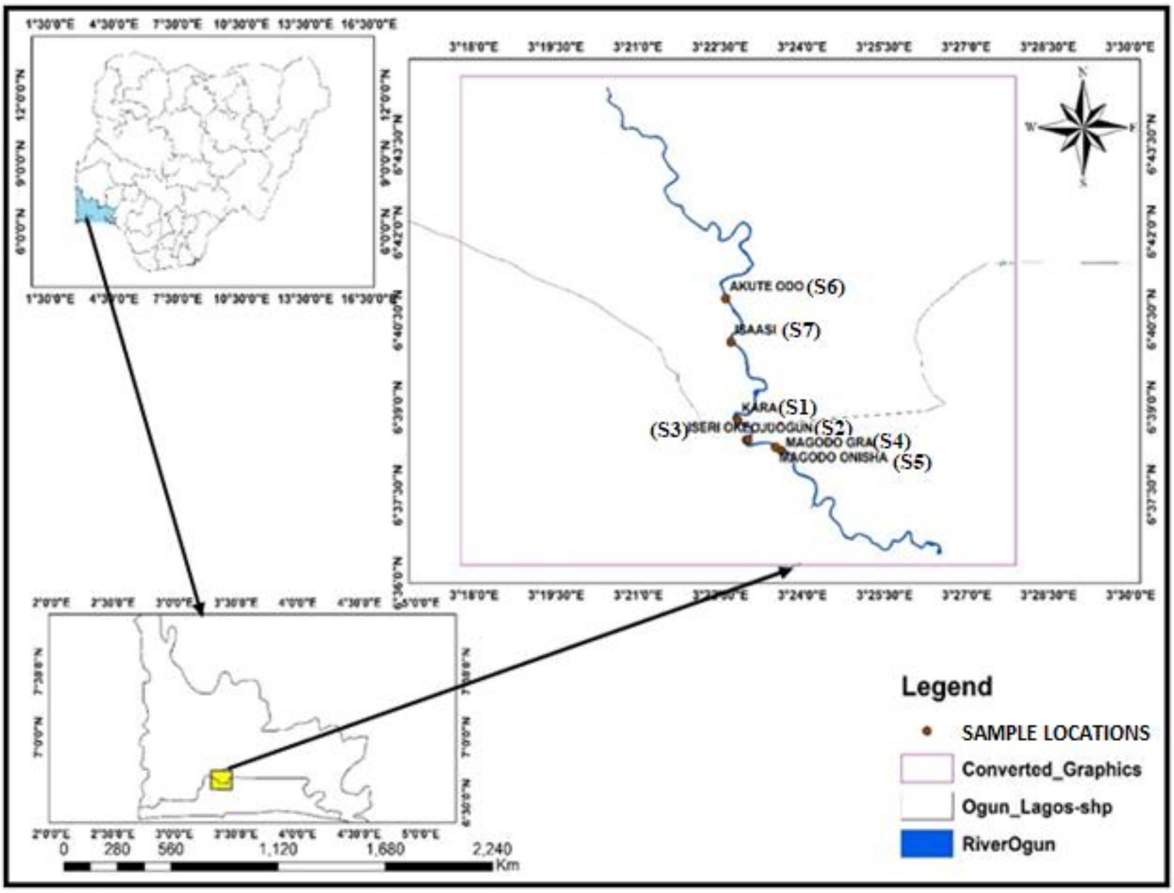

Figure 1. Map of Ogun River showing the Sampling Locations

2. Materials and Methods

2.1 Sampling and Sample Pretreatment

A portable Global Positioning System (GPS, GARMIN eTrex 10) measured the coordinates of each sampling point, which was further used to map the sampling area (Figure 1). Seven coastal sediment samples were collected along Ogun River waterways at 50 m intervals at 10 ± 1 m depth. The samples were stored in pre-cleaned, black polythene bags. Also, the geology, physical structures, and human activities around the sampling locations were observed.

Next, the samples were air-dried naturally for three weeks, by which time a constant weight was observed. Then, they were grounded and sieved to <2 µm particle size. The analysis was carried out during the day using the standard procedures of Watts and Johnson, 2012. The bulk Ni, Zn, Co, Mn, Fe, Pb, Cd, Cr, and Cu concentrations were first determined as follows: 5 g of the sediment sample was added to 100 ml of 2 M aqua regia in a 250 mL beaker. The mixture was gently heated on an electric hot plate to 105 ^{o}C for 2 h. Then, it was allowed to cool to room temperature before the volume was made to mark with distilled water (Pal & Tarafdar, 2009). The bulk metal concentration was determined using Atomic Absorption Spectrophotometer (AAS, Buck Scientific Model 205A). We further carried out sequential extraction (Section 3.2) to determine the metals' geochemical forms using the same AAS instrument.

2.2 Sequential Extraction Techniques

The schematic representation of sequential extraction used for this study is depicted in **Figure 2**. In this method, the trace metals were separated into five operationally defined fractions, namely exchangeable (F1), carbonate-bound (F2), Fe-Mn oxide-bound (F3), organic matter-bound (F4), and residual fraction (F5) (Aiyesanmi *et al*., 2020; Akinnawo et al. 2015; Rauret et al., 1989). This method was the modification of Tessier *et al.* (1979).

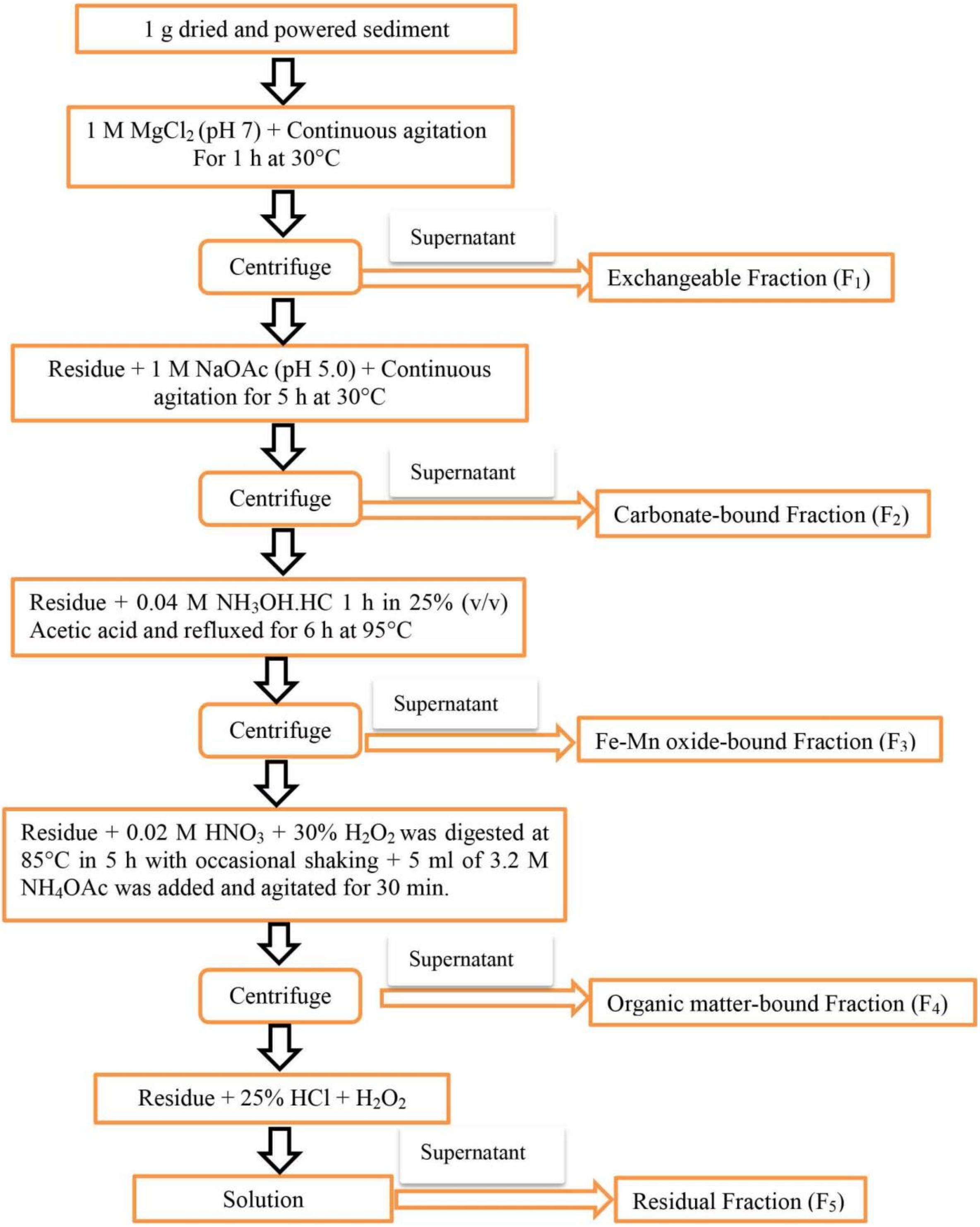

Figure 2. A Flow Chat of the Sequential Extraction Procedure for the Trace Metals in the Sediment Samples (Akinnawo *et al. 2015*)

3. Results and Discussion

3.1 Field Observation of Sampling Sites and Samples

Table 1 presents the field data and description of samples collected for this study. Seven coastal sediment samples were randomly collected, considering the geographical position of each sampling location. The color of the sediments varies and ranges from brownish grey, dark grey, brownish, to brownish grey. The color variation could result from the decomposition of silicate minerals or the oxidation and reduction of some metallic elements therein. Moreover, the texture varies from coarse sandy, sandy, very fine silt, silt clay, fine silt, to silt. These textural discrepancies could be ascribed to the different sedimentation rates of the soils or the turbidity currents due to deposition. Sediment samples were collected where active human activities (such as abattoirs, settlement areas, sewage disposal spots, and local dredging sites) prevailed.

3.2 Bulk Concentration and Geochemical Speciation of the Toxic Metals in the Sediment Samples

Using Microsoft Excel 2019 software, we computed the bulk metal concentrations obtained from the wet digested samples in **Table 2**. All the metals, except Zn, existed in concentrations much above the permissible limits in sediments (Ideriah et al., 2012). We observed that the metal concentrations followed the trend: Fe >> Mn > Zn > Pb > Co >> Cu ≈ Cr ≈Ni >> Cd. While by location, S_3 and S_6 were highly polluted than the other sites, likely due to the long-term, intense, and incessant anthropogenic activities associated with the sites. **Fig. 3** graphs were obtained to depict the descriptive data of the various geochemical forms observed for each sample.

3.2.1 Exchangeable Fraction (F_1)

Exchangeable fractions are weakly bound metals, readily bioavailable on the surfaces of soil and sediment grains because of the weak electrostatic interactions and ion-exchange processes (Samhan et al., 2014). The F_1 can be released into the environment under acidic conditions, thereby endangering the environment (Aiyesanmi et al., 2020; Al-mur, 2019; Bakircioglu et al., 2011). The range and average of released trace metals in F1 varied, as depicted in **Fig. 3a**. Fe and Mn have the highest values, followed by Pb, Cr, Co, and Cd, while Cu was the lowest. However, the F_1 concentrations of Cr, Cd, and Cu are low, indicating their high potential mobility, ecological bioavailability, and health risks. Thus, they require utmost attention for remediation or avoidance.

3.2.2 Carbonate-Bound Fraction (F_2)

The F_2 fractions are shown in **Figure 3b**. Like F_1, Fe existed more in the carbonate form than the other metals. It has been reported that trace metals extracted from soils/sediments with sodium acetate (1 M, pH 5) might be absorbed by low-energy sites on clay minerals, organic matter, and oxide minerals (Aiyesanmi et al., 2020; Al-mur, 2019; GIeyzes et al., 2002). Therefore, toxic metals recovered in this fraction are refractory and can be released in mildly acidic conditions (pH < 5), making them potentially bioavailable. Although the F_2 species are relatively stable and poorly leachable, Fe, Mn, Zn, and Cu exert environmental risks to the studied area.

Table 1. Field Data and Description of Samples

Sample ID	Sample location	Latitude	Longitude	Color	Texture	Field observation
S1	Kara	6◦38'47.0"N	3◦22'48.7"E	Whitish grey	Very fine silt	Presence of industrial jetty, abattoir market
S2	Ojuogun	6◦38'26.5"N	3◦22'58.2"E	Brownish	Coarse sandy	Terrestrial activities, fishing, urban settlement, local dredging
S3	Iseri Oke	6◦38'26.8"N	3◦23'00.5"E	Whitish grey	Very fine silt	Terrestrial activities fishing, urban settlement, local dredging
S4	Magodo GRA	6◦38'15.5"N	3◦23'36.9"E	Dark grey	Silt	Energy industrial sewage discharge
S5	Magodo Onisha	6◦38'19.4"N	3◦23'29.9"E	Brownish grey	Sandy	Sewage discharge terrestrial, activities fishing, urban settlement
S6	Akute Odo	6◦40'52.0"N	3◦22'35.8"E	Dark grey	Silt clay	Local dredging activities, fishing, sewage discharge, and dense house settlement
S7	Isaasi	6◦40'07.3"N	3◦22'41.3"E	Brownish grey	Fine silt	Local dredging activities, fishing, sewage discharge

Table 2. Bulk Concentrations of the Trace Metals (in ppm) in the Sediments from the Various Sampling Locations

Sample ID	Ni (ppm)	Zn (ppm)	Co (ppm)	Mn (ppm)	Fe (ppm)	Pb (ppm)	Cr (ppm)	Cd (ppm)	Cu (ppm)
S1	22.36	180.3	116.7	390.6	1122	203.0	30.24	3.335	31.09
S2	28.03	283.1	124.2	490.1	1120	202.1	27.49	3.724	33.78
S3	32.69	462.3	240.1	878.0	2242	405.7	57.83	6.853	64.47
S4	82.28	264.4	173.5	403.4	1190	189.3	34.01	3.798	34.99
S5	27.94	186.5	83.74	394.3	1205	153.9	37.82	4.154	32.82
S6	29.59	450.6	256.9	795.7	2393	342.4	71.83	7.643	67.71
S7	57.23	345.5	90.93	467.9	1111	187.3	36.68	4.261	30.11

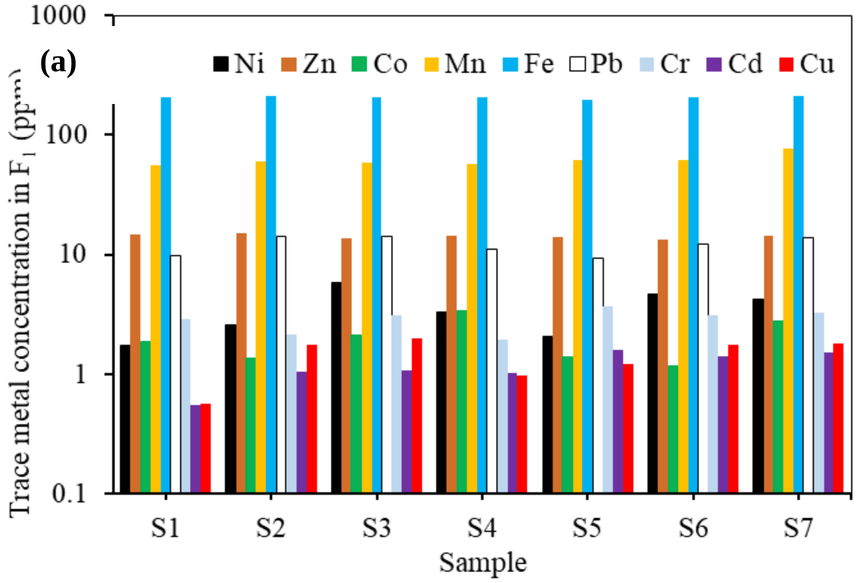
(a)
■Ni ■Zn ■Co ■Mn ■Fe □Pb ■Cr ■Cd ■Cu
Trace metal concentration in F_1 (pp
1000
100
10
1
0.1
S1
S2
S3
S4
S5
S6
S7
Sample

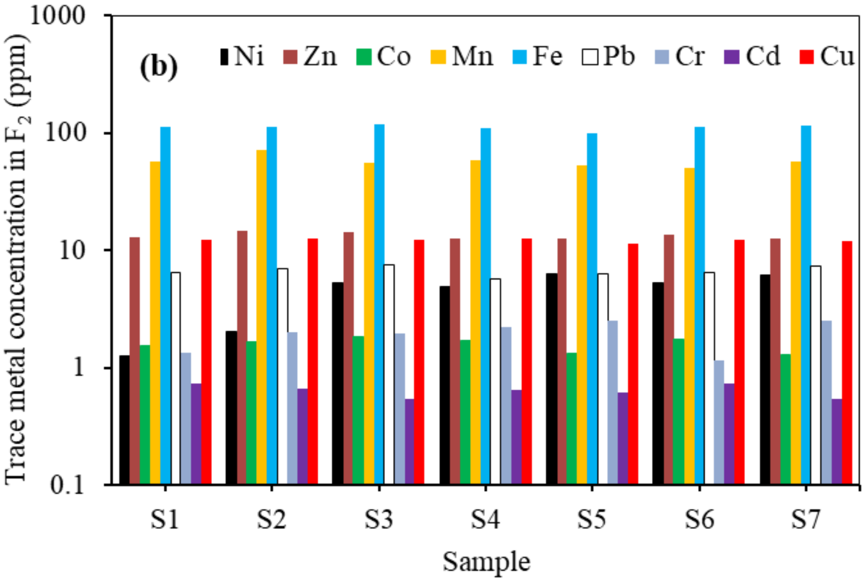
(b)
■Ni ■Zn ■Co ■Mn ■Fe □Pb ■Cr ■Cd ■Cu
Trace metal concentration in F_2 (ppm)
1000
100
10
1
0.1
S1
S2
S3
S4
S5
S6
S7
Sample

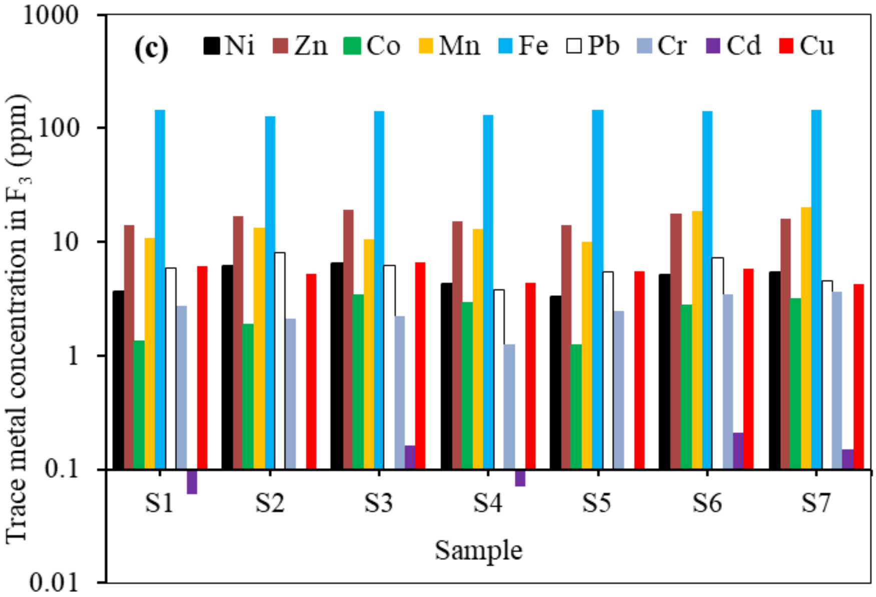
(c)
Ni
Zn
Co
Mn
Fe
Pb
Cr
Cd
Cu
Trace metal concentration in F$_3$ (ppm)
1000
100
10
1
0.1
0.01
S1
S2
S3
S4
S5
S6
S7
Sample

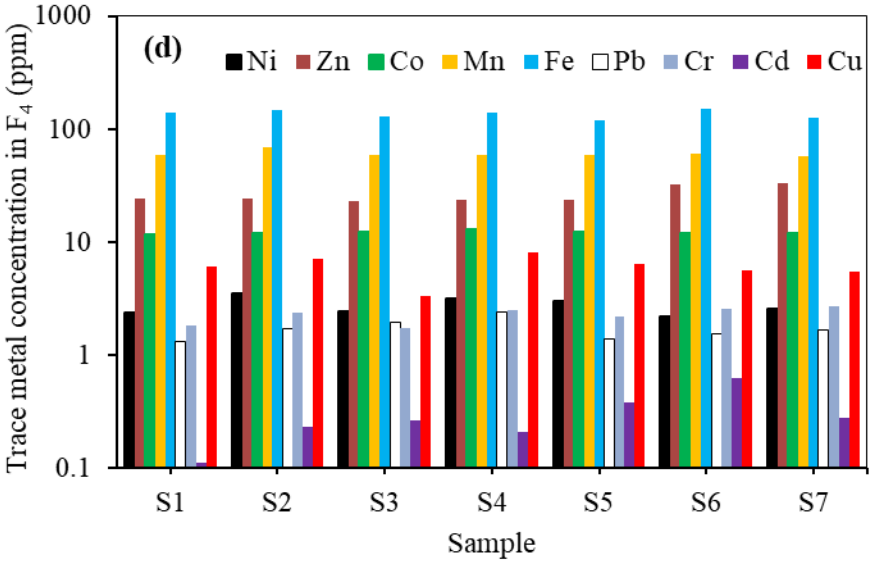
(d)
Ni
Zn
Co
Mn
Fe
Pb
Cr
Cd
Cu
Trace metal concentration in F$_4$ (ppm)
1000
100
10
1
0.1
S1
S2
S3
S4
S5
S6
S7
Sample

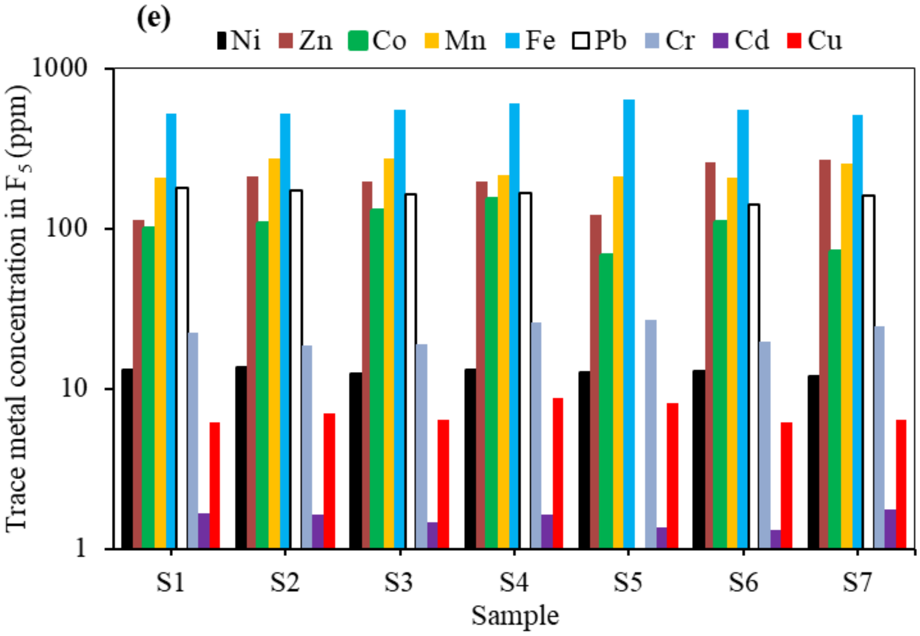

Figure 3. Graphical Representation of toxic Metal Concentrations in (a) Exchangeable (F_1), (b) Carbonate-Bound (F_2), (c) Fe-Mn Oxide-Bound (F_3), (d) Organic-Bound (F_4), and (e) Residual (F_5) Phases

3.2.3 Reducible Fraction (F_3)

This fraction is bound to the hydrous oxides of Mn and Fe. The species are released into the environment under a reducing conditions. In the current study, the F_3 abundance follows the trend: Fe, Zn, Mn, Pb. However, Co, Cr, and Cu were low (**Figure 3c**). Generally, *F*3 is relatively stable (slowly mobile and poorly available) but could change with variation in redox conditions, becoming more and less soluble under reducing and oxidizing conditions, respectively (Aiyesanmi et al., 2020; Al-mur 2019; Egila & Nimyeh, 2002). Because metal mobility influences toxicity, an increase in reducing conditions in the soil could increase a metal's toxicity. Therefore, the F_3 pattern suggests high Fe bioavailability in the soil.

3.2.4 Organic Fraction (F_4)

Here, we observed high Fe concentration in the samples. Smaller fractions of Pb and Cd were also noted (**Figure 3d**). The F_4 is released in sediment under strongly oxidizing conditions and, consequently, is an essential source of potentially available trace metals (Doddaiah et al., 2012). However, organic fractions are neither mobile nor readily available. Because of their association with high molecular weight substances, F_4 could be released in small quantities into the environment.

4.2.5 Residual Fraction (F_5)

The highest Fe concentrations occurred in the residual fraction, followed by Mn, Pb, Zn, and Co concentrations (**Figure 3e**). This observation implies that the metals are firmly bound to the sediments. Also, the high Fe levels in this inert phase correspond to the immobilized, refractory geochemical forms

(Aiyesanmi et al., 2020; Doddaiah et al., 2012). However, the significant increase in Fe concentration in the F_5 is likely ascribed to anthropogenic sources. Since the residual fractions are predominant for the toxic metals, they are firmly bounded within their crystal structure and are not readily released into the environment. Hence, they have low mobility and low bioavailability. Therefore, a large proportion of the toxic metals are environmentally benign.

In addition, the study compared its findings with other previous literature and discovered that recent findings contradicted previous work in the study area, which dwelled on the bioavailability of heavy metals without taking into consideration the bio-diversity and bioaccumulation, which correlates with the findings of Olumayede and Ediagbuya, 2018; Helen and Okeme, 2021; Ghafar and Hikmat, 2018; Zayeng *et al*., 2022; Li *et al*., 2019; Sadiq *et al*., 2016 amongst others

3.3 Spatial Distribution of theToxic Metals' Geochemical Phases

The relative fractional distribution of the toxic metals was further analyzed using ArcGIS 10.3 to generate cartographic maps (**Figure 3**). Considering the environmental toxicity and bioavailability of the phases, the decreasing trend of green depth (from light to deep green) on the cartographic map denotes areas with very low (through moderate and high) to very high toxicity, based on their geochemical phases.

3.3.1Ni

In low concentrations, nickel is usually found in soils, water, air, and sediments. However, **Figure 3a** shows that its distribution in the study area was relatively high, especially in the residual fraction. The relatively bioavailable fractions predominated in the northern half of the study area. Ni originates from various industrial practices and wastewaters of catalyst, pigment, and dry-cell electrode factories. Ni-bearing scums from wastewater treatment are often dumped into the ocean and landfills. The vast anthropogenic sources of Ni in the studied area could be attributed to nickel wood, fuel combustion, agricultural wastes, domestic sludge, atmospheric deposition, river runoffs, industrial effluents, and municipal discharges. Similarly, the natural erosion of soils and rocks may contribute to its environmental dispersion. If environmental available, Ni consumption could cause chronic bronchitis and lung cancer.

3.3.2Zn

Zn distribution in the study area ranged from deep to light green (**Figure 3b**). The distribution followed the order: residual > organic > reducible > exchangeable > carbonate. Unlike Ni, the northern hemisphere of the study region is characterized by residual fractions, indicating more benign fractions of Zn therein. Studies have suggested that Zn is highly mobile in the environment, and its bioavailability increases in the ionic form (Zn^{2+}). Its distribution in the sediment is attributed to emissions from waterway transportation engines, household roofing sheets, commercial activities, and industrial discharge. However, over accumulation of Zn in the human body causes nausea, vomiting, loss of appetite, and stomach cramps.

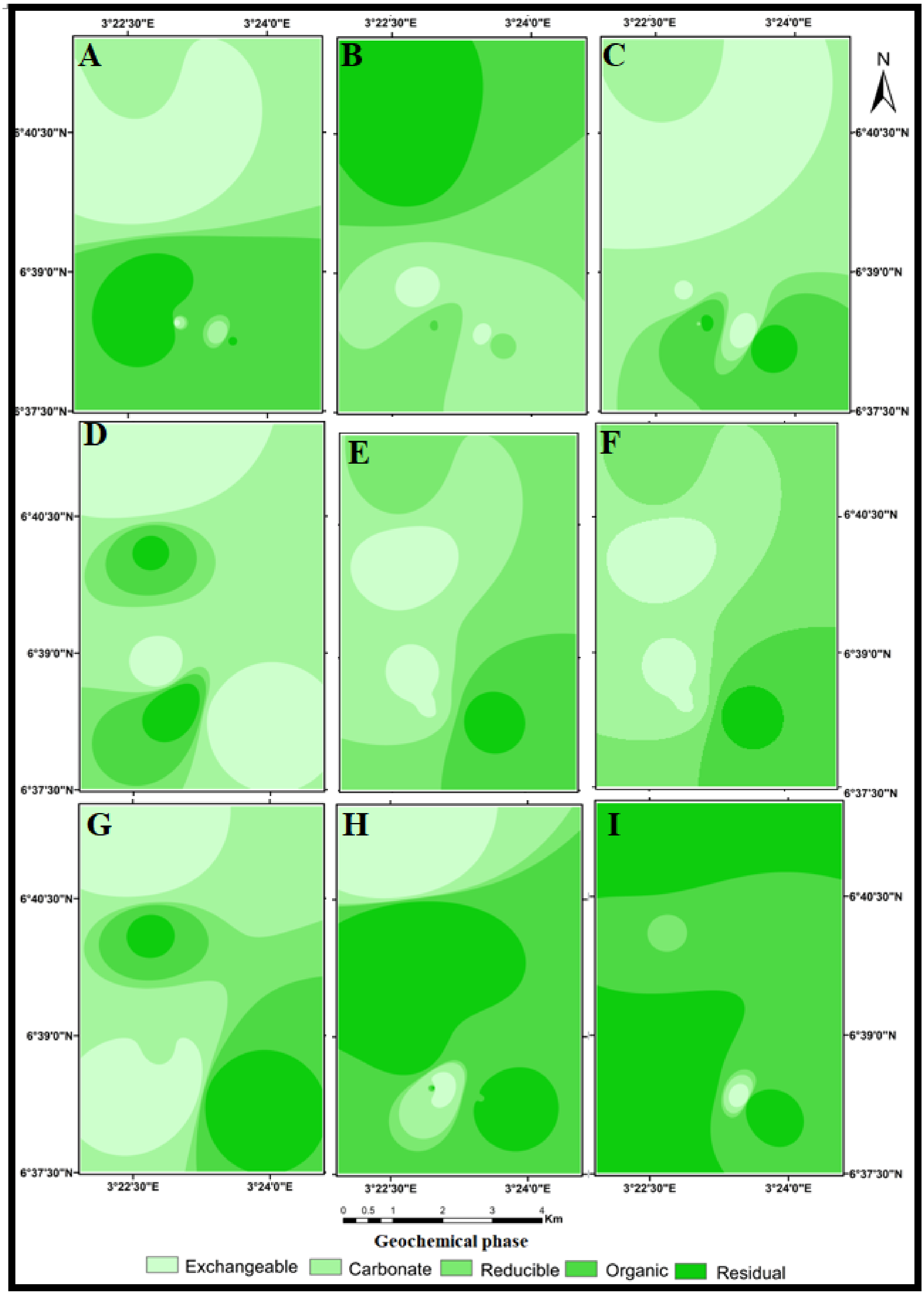

Figure 4. Geospatial Cartography Showing the Geochemical Distribution of (a) Ni, (b) Zn, (c) Co, (d) Mn, (e) Fe, (f) Pb, (g) Cr, (h) Cd, and (i) Cu in the Study Area

3.3.3 Co

Co was predominant in the residual fraction, followed by the organic fraction (**Figure 4c**). The high Co concentration in the studied area could be ascribed to the industrial sewage discharge therein. The south-eastern area of the region is predominated with refractory fraction. Therefore, this location is relatively safe from Co toxicity. Co causes skin irritation and rashes, nausea, and vomiting at excess levels in the human body. Therefore, residents of the northeast of the Ogun River are at higher risk of cobalt poisoning.

3.3.4 Mn

The Mn distribution in the studied area is cartographically presented in **Fiure 4d**. The distribution range was dispersed across the geochemical forms. The residual fraction was concentrated in the west and southwest regions. The highest distribution of Mn could result from natural atmospheric deposition and decomposition of organic matter deposited via anthropogenic activities, such as indiscriminate waste disposal from nearby abattoirs, markets, and industries. However, Mn toxicity can induce a permanent nervous disorder, leading to tremors and facial muscle spasms in exposed humans**.**

3.3.5 Fe & Pb

The spatial descriptions of Fe and Pb in the studied area are identical (**Figures 4d** and **4e**). Fe level was excessively high in all fractions, following the order: residual > exchangeable > reducible > organic > carbonate. Those of Pb followed the same sequence but in lesser concentrations. The high Fe concentrations could be attributed to weathering, alteration, and transportation of Fe-bearing minerals (such as micas and feldspars) into the sediments. Besides the natural sources, anthropogenic activities (such as industrial jetty waste disposal, abattoir market, fishing, waterways transportation, terrestrial activities, local dredging, and indiscriminate municipal waste disposal) contribute to the Fe pollution around the northeast Ogun River. On the contrary, the presence of Pb in the sediments could be attributed to anthropogenic activities, especially indiscriminate industrial discharge and waste disposal from the vicinity. Therefore, bio-accumulated and biomagnified Fe via the food chain can be assimilated by humans, resulting in health risks. Excessive Fe ingestion may lead to constipation, diarrhea, nausea, and vomiting in the people living around the studied area. And, with the highest concentration of Pb found in the reducible fraction, Pb toxicity in humans could cause intestinal cancer, lung cancer, and central nervous system breakdown.

3.3.6 Cr

Basically, Cr is high in the residual fraction, followed by the exchangeable fraction. The abundance of Cr in the residual fraction implies low mobility and bioavailability of the metal in the study area, thus, posing the least environmental threat. Overall, Cr distribution in the sediment varies adequately across the fractions (**Fig. 4f**). Generally, the distribution of Cr in the samples followed the order: residual > exchangeable > reducible > organic > carbonate.

3.3.7Cd

Cadmium is the least abundant toxic metal in the sediments of the studied area and is predominant in the residual fraction (**Fig. 4g**). It is opined that the metal gets into the surface water due to the dispersion of paints and coloring from nearby road surfaces. Cd is more mobile in the waterway body than other metals. Hence, it is potentially more persistent in the water and sediment. Therefore, the metal must be remediated because of its inherent toxicity if it is impossible to avoid the proximity to the vicinity.

3.3.8 Cu

Copper is predominant in the exchangeable fraction (**Fig. 4h**); following the order: exchangeable > carbonate > residual > organic > reducible. Therefore, Cu in the sediment samples may be attributed to anthropogenic activities from residents around the northeast of the river, such as industrial sewage discharge loaded with various metal-rich wastes and domestic waste containing Cu. However, the excessive ingestion of Cu causes headaches, fever, liver and kidney damage, and intestinal irritation.

These high relative distributions could be attributed to various anthropogenic activities, especially those residing at the northeast of the Ogun River and geogenic from underlying crystalline rocks. However, since Cd is geochemically bioavailable in all the geochemical phases, it has more severe effects on humans and aquatic lives as it can cause sudden death, excessive bleeding, and mortality if consumed through food crops and marine mammals and poses a severe threat to the well-being of the inhabitants, especially infants, mothers, and elderly residents. Also, the abundance of Fe could be attributed to the tropical weathering of the crystalline rocks and the release of the minerals into nearby streams and rivers. Other metals (such as Cu, Zn, and Pb) may also coagulate to form mineral deposits from which certain ores can be extracted, such as chalcopyrite ($CuFeS_2$), and Smithsonite (ZnS) or Galena (PbS) through supergene enrichment.

3.4 Statistical Correlation

The five metal speciation fractions were further subjected to the inter-metal association via Spearman's rank correlation. The results for F_1 are shown in **Table 3**. Examples of major pairs of metals are Ni/Zn, Ni/Co, Ni/Pb, Ni/Cd, Ni/Cr, and N/Cu. Other pairs are Zn/Pb, Zn/Cd, Co/Pb, Co/Cd, and Cd/Cu, and all show strong correlations. Strong correlations signify that each paired metals have a common contamination source.

The Spearman's rho correlation indicates that the metals are highly positively correlated and associated, implying that they are of the same source of enrichment (anthropogenic process). The component plots of the metals for F_1 showed two components (**Figure 4a**) where the metals clustered into component 1, indicating that the metals have a common source of origin.

Table 3. Correlation Coefficient of Metals in F_1

	Ni	Zn	Co	Mn	Fe	Pb	Cr	Cd	Cu
Ni	1.000								
Zn	0.905**	1.000							
Co	0.973**	0.844*	1.000						
Mn	0.724*	0.600	0.663	1.000					
Fe	-0.515	-0.569	-0.309	-0.569	1.000				
Pb	0.991**	0.896**	0.991**	0.657	-0.408	1.000			
Cr	0.895**	0.732	0.817*	0.732	-0.661	0.849*	1.000		
Cd	0.991**	0.896**	0.991**	0.657	-0.408	1.000*	0.849*	1.000	
Cu	0.895**	0.824*	0.895**	0.560	-0.450	0.906**	0.745	0.906**	1.000

**. Correlation is significant at the 0.01 level (2-tailed).

*. Correlation is significant at the 0.05 level (2-tailed).

Table 4 shows the correlation coefficient of metals in F_2 of the studied area. The inter-metal association is evaluated by Spearman's rank correlation (ῤ), showing some major pairs of the metals. Ni is strongly correlated with Co and Pb. Co is strongly correlated with Pb and Cr, while Pb is related to Cr. Strong correlations signify that each paired metals have a common contamination source. The Spearman's rho correlation indicates that the metals are highly positively correlated and associated, implying that they are of the same source of enrichment (anthropogenic process). The principal component analysis shows the metals in three components.

Table 4. Correlation Coefficient of Metals in F_2 Studied Area

	Ni	Zn	Co	Mn	Fe	Pb	Cr	Cd	Cu
Ni	1.000								
Zn	0.626	1.000							
Co	0.914**	0.563	1.000						
Mn	0.505	0.732	0.654	1.000					
Fe	-0.497	-0.617	-0.163	-0.171	1.000				
Pb	0.925**	0.482	0.945**	0.525	-0.319	1.000			
Cr	0.626	0.600	0. 809*	0.732	-0.880*	0.784*	1.000		
Cd	-0.954**	-0.418	-0.918**	-0.386	0.316	-955**	0. 657	1.000	
Cu	0.535	-0.144	0.315	-0.441	-0.258	0.412	-0.114	-0.612	1.000

**. Correlation is significant at the 0.01 level (2-tailed).

*. Correlation is significant at the 0.05 level (2-tailed).

The Spearman’s rho correlation for F_3 (**Table 5**) indicates that the metals are highly positively correlated and associated, implying that they are of the same source of enrichment (anthropogenic process).

Table 5. Correlation Coefficient of Metals in F3 Studied Area

	Ni	Zn	Co	Mn	Fe	Pb	Cr	Cd	Cu
Ni	1.000								
Zn	0.991**	1.000							
Co	0.981**	0.991**	1.000						
Mn	0.882**	0.874*	0.882**	1.000					
Fe	0.802**	0.872*	0.882**	0.000	1.000				
Pb	0.946**	0.955**	0.927**	0.722	0.982**	1.000			
Cr	0.963**	0.954**	0.963**	0.890**	0. 889**	0.000	1.000		
Cd	0.973**	0.982**	0. 963**	0.801*	0.901*	0.945**	0.000	1.000 .	
Cu	0.981**	0.991**	0.972**	0.808*	0.982**	0.925	0.991**	1.000	

**. Correlation is significant at the 0.01 level (2-tailed).

*. Correlation is significant at the 0.05 level (2-tailed).

Table 6. Correlation Co-Efficient of Metals in F_4 Studied Area

	Ni	Zn	Co	Mn	Fe	Pb	Cr	Cd	Cu
Ni	1.000								
Zn	0.930**	1.000							
Co	0.905**	0.860*	1.000						
Mn	0.569	0.635	0.618	1.000					
Fe	0.000	0.000	0.000	0.000	1.000				
Pb	0.930**	0.846*	0.972**	0.635	0.000	1.000			
Cr	0.725	0.749	0.655	0.471	0. 000	0.749	1.000		
Cd	0.905**	0.935**	0. 973**	0.618	0.000	0.935**	0.728	1.000	
Cu	0.905**	0.935**	0.973**	0.618	0.000	0.935**	0.728	1.000	

**. Correlation is significant at the 0.01 level (2-tailed).

*. Correlation is significant at the 0.05 level (2-tailed).

Table 7 shows that Ni strongly correlates with Zn and mildly with Co, Mn, and Pb. Zn pairs with Co, Mn, Pb and Cu. Co has a strong correlation with Mn and Cu. Mn pairs strongly with Pb and Cu.

Table 7. Correlation Coefficient of Metals in Residual Fraction (F_5)

	Ni	Zn	Co	Mn	Fe	Pb	Cr	Cd	Cu
Ni	1.000								
Zn	0.905**	1.000							
Co	0.896**	0.991*	1.000						
Mn	0.870*	0.982**	0.973**	1.000					
Fe	0.683	0.618	0.612	0.525	1.000				
Pb	0.896**	0.991**	1.000**	0.973**	0.612	1.000			
Cr	0.000	0.000	0.000	0.000	0. 000	0.000	1.000		
Cd	0.896**	0.955**	0. 929**	0.918**	0.929**	0.000	1.000	1.000 .	
Cu	0.725	0.915**	0.906**	0.911**	0.676	0.906**	0.000	0.867	1.000

**. Correlation is significant at the 0.01 level (2-tailed).

*. Correlation is significant at the 0.05 level (2-tailed).

The extraction method of component analysis shows that component 1 environment (**Table 8**) has Co and Pb as strong polluting metals that are lethal. The principal component analysis for F_1 showed the abundance of all the metals except Fe in component one (1). The Fe (-553) is strongly depleted in component one and strongly enriched in component two (2). For F_2, the first component shows an abundance of Ni, Co, Pb, and Cr, while components two and three are negatively and strongly depleted in the areas. There is also a pronounced depletion of metals (like Cd) in component 1 and Cu in component 2. The component plots in the rotated space (**Fig. 4b**) show the metals clustering into component 3, indicating that the metals have a common source of origin except for Cd and Fe, which fell into components 2 and 1, respectively. The component plots of the metals for F_3 showed two components (**Fig. 4c**) where the metals clustered into component 1, indicating that the metals have a common source of origin. The principal component analysis in Table 8 for F_3 showed the abundance of all the metals except the Fe in component one (1). The Fe (-553) is strongly depleted in component one and strongly enriched in component two (2).

Regarding F_4, Ni is strongly and positively correlated with Co, Pb, Cd, and Cu. Zn is associated with Cd and Cu. Other pairs are Co/Pb, Co/Cd, Co/Cu, Pb/Cd, and Pb/Cu. The principal component analysis shows that component 1 has a strong positive correlation of Ni, Co, and Pb and a very strong negative Cd from the extraction method. Components 2 and 3 are depleted of almost all the metals. In consonance with the abundance of the metals, the component plot in rotated space (Fig. 4d) explains the clustering of the metals in component 3 just like the metals in $F_{1,}$ implying a common concentrated pollution source. Components 2 and 3 of F_5 are strongly depleted of Fe and Cu, respectively, indicating that they may not have any consequential impact on the environment. The component plot in rotated space (Fig. 4e) also sees the clustering of the metals in component 3. Generally, the component 3 environment from all the sampled areas is highly susceptible to pollution.

Table 8. Component Matrix of Principal Component Analysis Using Extraction Method

Metal	**F_1 component**		**F_2 component**			**F_3 component**		**F_4 component**			**F_5 component**		
Ni	.984	0.68	.944	-1.5	-.01	.984	.068	.944	-.15	-.01	.871	.381	-.10
Zn	.926	-.01	.800	3	0	.926	-.01	.800	3	0	.564	.698	5
Co	.950	9	.925	.253	-.46	.650	9	.925	.253	-.46	.974	.068	.339
Mn	.771	.155	.760	-.04	5	.771	.155	.760	-.04	5	.700	.216	-.03
Fe	-553	-.19	-.44	8	.310	-.55	-.19	-.44	8	.310	-.10	-.96	6
Pb	.965	2	7	.599	.002	3	2	7	.599	-.00	0	4	.631
Cr	.884	.794	.903	.257	.834	.965	.794	.903	.257	2	.902	.211	.145
Cd	.893	.137	.846	-.26	.172	.884	.137	.846	-.26	.834	.868	.073	-.23
Cu	.858	-.32	-.92	2	.229	.893	-.32	-.92	2	.172	-.89	-.26	5
		7	3	.289	-.10	.858	7	3	.289	.229	6	6	.303
		.412	.211	.169	9		.412	.211	.169	-.10	.233	.112	.135
		.209		-.96	.088		.209		-.96	9			-.96
				8					8	.088			0
	2components extracted		3 components extracted			2components extracted		3 components extracted			3 components extracted		

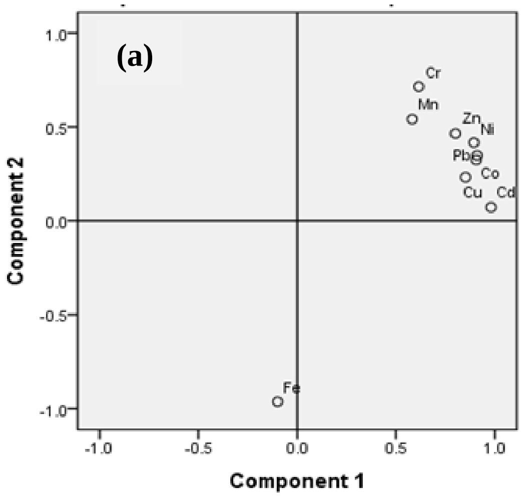

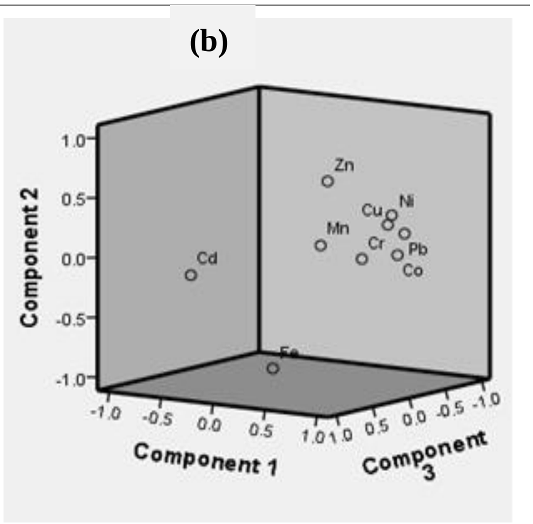

(c)

(d)

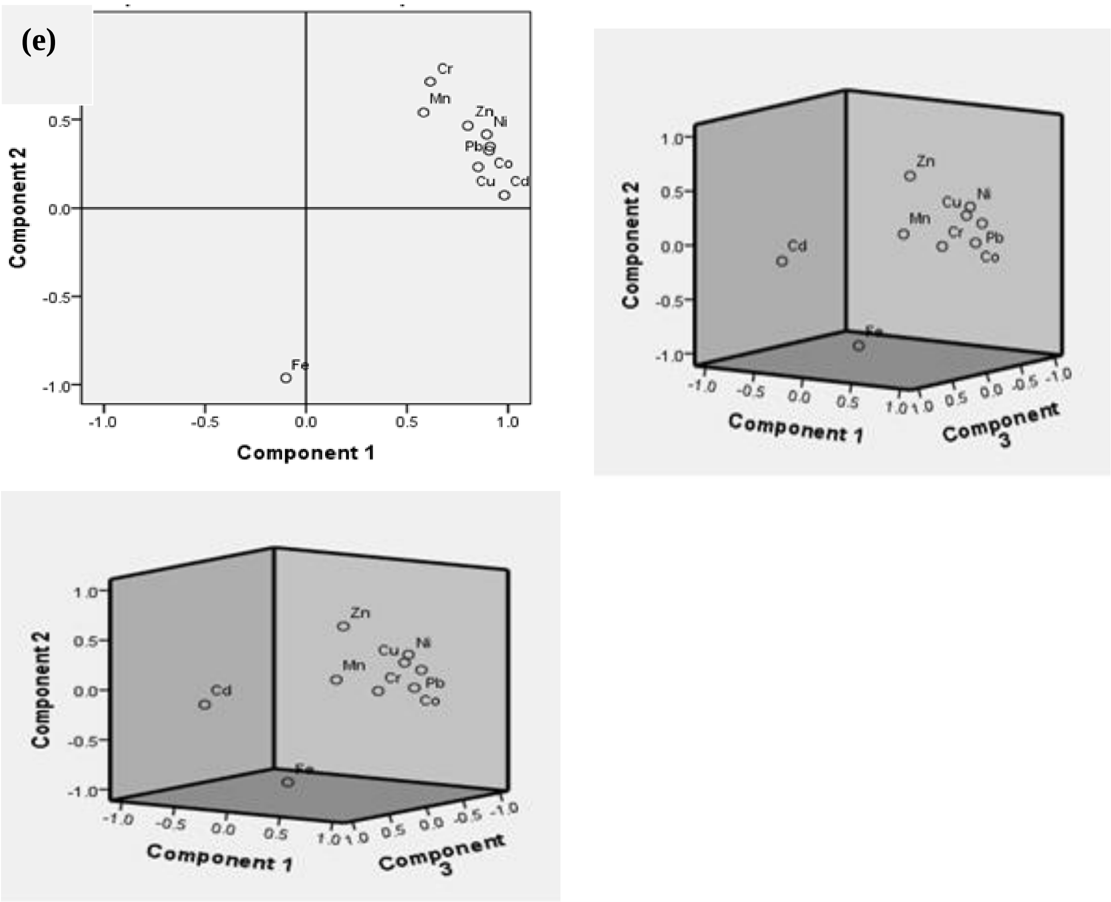

Fig. 4. Component plot in rotated space for (a) F_1, (b) F_2, (c) F_3, (d) F_4, and (e) F_5

4. Conclusions and Recommendations

The sequential extraction of toxic metals in the sediments sampled from the study area uncovered the geochemical nature of Cd, Cu, Mn, Fe, Pb, Zn, Ni, Cr, and Co. Arsenic (As) was not determined because the analysis equipment was incompatible with the analyte, i.e., because of its relative volatility, shared with Hg. Aside from Zn, all the metals existed at levels much above the permissible limits in sediments. The bulk metal concentrations followed the trend: Fe >> Mn > Zn > Pb > Co >> Cu ≈ Cr ≈Ni >> Cd. Overall, the highest proportions of the metals exist as a residual fraction. Thus, they are firmly bounded within their crystalline structure and not easily released into the environment. However, relatively high concentrations of Fe, Mn, Zn, Pb, and Co were found in the bioavailable phase. Generally, Cd and Fe showed the least and highest distributions of the geochemical forms in the sediments, respectively.

Therefore, proper monitoring of the level of toxic metals should be done, and human awareness regarding the toxic properties of the metals be made to the people in this community. In addition, industries and abattoirs should be adequately monitored, and strict regulations imposed on the Industries on proper discharges of industrial effluents. However, all these toxic metals have potential and long-term chronic effects on exposure, such as mutations or deformities. Monitoring toxic metals levels in the sediment and water becomes imperative to prevent excessive buildup of these metals in humans through food chains.

Disclosure statement

Conflict of Interest: The authors declare no conflicts of interest.

Compliance with Ethical Standards: Not applicable.

Consent to Participate: This article does not involve any human subjects.

Consent to Publish: Not applicable. All manuscript data, figures, and tables are original to this study.

Funding: This research was not funded by any person or organization.

Authors' contributions

OSA conceived, supervised, and organized the study; AAA co-supervised, organized the write-up, and did the editorials; DRK carried out the lab experiment with OSA and the geospatial analysis with AAA; HYM and RYO carried out the statistical analyses.

References

Akinnawo, S., Olajide, A., & Olanipekun, E. (2015). Ecological risk assessment and contamination levels of heavy metals and Pesticide Residues in Water and Sediment from Ondo Coastal Region, Nigeria. *Asian Journal of Science and Technology*, *7*(1), 2169-2179.

Al-Mur, B. A. (2019). Geochemical fractionation of heavy metals in sediments of the Red sea, Saudi Arabia. *Oceanologia*, *62*(1), 31-44. https://doi.org/10.1016/j.oceano.2019.07.001

Aiyesanmi, A. F., Oladele, M. F., Adelodun, A. A., & Idowu, G. A. (2020). Speciation and bioavailability studies of toxic metals in the alluvial soil of Onukun River floodplain in Okitipupa, Southwestern Nigeria. *Environmental Quality Management*, *30*(2), 131-143. https://doi.org/10.1002/tqem.21720

Ayodele, O. S., Henry, Y. M., & Fatoyinbo, I. O. (2019). Heavy metals concentration and pollution assessment of the beach sediments in Lagos, Southwestern Nigeria. *SDRP Journal of Earth Sciences & Environmental Studies*, *4*(2), 567-578.

Ayodele, O. S., Madukwe, H. Y., & Adelodun, A. A. (2021). Geoenvironmental evaluation of toxic metals in the sediments of Araromi Coastal Area, Southwestern Nigeria. *Journal of Environmental Quality and Management* (Willey), 2021, 1-19.

Bakircioglu, D., Kurtulus, Y. B., & Ibar, H. (2011). Investigation of trace elements in agricultural soils by BCR sequential extraction method and its transfer to wheat plants. *Environmental Monitoring Assessment*, *175*, 303-314. https://doi.org/10.1007/s10661-010-1513-5

Chukwuka, K. S. (2011). Utilization of aquatic mariophyte in Nigerian freshwater. *Journal of Fisheries and Aquatic Science*, *6*(5), 490-496. https://doi.org/10.3923/jfas.2011.490.498

Ditholong, L., Matabene, T. W., Godeto, R., Manpa, M., & Abaynah, A. (2021). Sequential extraction and risk assessment of potentially toxic elements in River sediments. *Minerals*, *11*(8), 874. https://doi.org/10.3390/min11080874

Doddaiah, S., Shivanna, S., Swamy, S., & Budiguppe, M. K. (2012). Speciation and geochemical behaviour of heavymetals in industrial area soil of Mysore City, India. *Journal of Environmental Protection*, *3*, 1384-1392. https://doi.org/10.4236/jep.2012.310157

Egila, J. N., & Nimyeh, D. N. (2002). Determination of trace metal speciation in sediments from some dams. *Journal of Chemical Society of Nigeria*, *27*, 71-74.

Forstner U., & Wittmann G. T. W. (1987). In Metal pollution in the aquatic environment (p. 486). Spring Verlag Berlin Heidelberg, New York.

Ghafar Ebadi, A., & Hikmat, H. (2018). Physico-chemical Characterization of sediments from Tajan River Basin in the Northern Iran. *Toxicological and Environmental Chemistry*, *100*, 540-549. https://doi.org/10-1080/02772248.2018-1460929

Gathua, N. (2015). Gatuaganya residents decry pollution of Chania. *Geologica Beligica*, *13*(1), 37-47.

Gleyzes, C., Tellier, S., & Astruc, M. (2002). Fractionation studies of trace elements in contaminated soils and sediments: a review of sequential extraction procedures. Trac-Trend. *Analytical Chemisty 21*(6), 451-467. https://doi.org/10.1016/S0165-9936(02)00603-9

Hessouth, M. I, Pereora, J. J., & Farthangui, H. J. (1994). In *Hydrocarbon Prospect for Exploration and Production Report* (p. 88).

Ho, H. H., Swennen, R., & Van Damme, A. (2010). *Distribution and contamination status of heavy metals in estuarine sediments near Cua Ong Harbor*. Ha Long Bay, Viatinam. Retrieved from https://www.businesslist.co.ke/category/industrial-services/city:thika

Helen, A., & Okiemen, I. E. (2021). Sequential extraction and mobility factor of metals in the Urban Soil of Warri-Nigeria (A case study of the Environment of Esisi Open Dump). *Journal of Environmental Protection*, *12*, 196-208. https://doi.org/10.4236/jep.2021.123012

Ideriah, T. J. K., David-Omiema, S., & Oggomma, D. N. (2012). Distribution of heavy metals in water and sediment along Abonnema Shoreline, Nigeria. *Resources and Environment*, *2*(1), 33-40. https://doi.org/10.5923/j.re.20120201.05

Kelly, M. G., & Whitton, B. A. (1995). The trophic diatom index: A new index for monitoring eutrophication in the rivers. *Journal of Applied Phycology*, *7*, 433-444. https://doi.org/10.1007/BF00003802

Korfali, S. I., & Davies, B. E. (2004). Speciation of metals in sediment and water in a river underlain by limestone: role of carbonate species for purification capacity of rivers. *Advances in Environmental Research*, *8*, 599-612. https://doi.org/10.1016/S1093-0191(03)00033-9

Kotoky, P., Bora, B. J., & Baruah, N. K. (2003). Chemical fractionation of heavy metals in soils around oil Installations, Assam. *Chemical Speciation and Bioavailability*, *15*(4), 115-126. https://doi.org/10.3184/095422903782775181

Murtala, B. A., Abdul, W. P., & Akinyemi, A. A. (2012). Bioaccumulation of heavy metals in fish

(Hydrocynus forskahlii, Hypero pisus bebe ocidentalis and Claria gariepinius) organs in Downstream Ogun Coastal Water, Nigeria. *Journal of Agricultural Science*, *4*(11), 1-9. https://doi.org/10.5539/jas.v4n11p51

Muwanga, A. (1997). *Environmental impacts of copper mining at Kilembe, Uganda: A geochemical investigation of heavy metal pollution of drainage waters, stream, sediments and soils in the Kilembe valley in relation to mine waste disposal* (PhD, dissertation). Universitaet Braunschweig, Germany.

Nigeria Open Data Survey. (2014). *2009 Census Volume 1 Table 3 Rural and Urban Population*.

Okunlola, O. W., & Olatunji, A. S. (2017). Geochemical Assessment and Speciation of metals in sediments of Osun and Erinle Rivers, Southwestern Nigeria. *Arabian Journal of Geosciences* *10*(16), 366. https://doi.org/10.1007/s12517-017-3110-1

Olumayede, E. G., & Ediabouya, T. F. (2018). Sequential extraction and toxicity potential of trace metals absorbed into airborne particles in an urban atmosphere of Southern Nigeria. *Scientific World Journal*, 1-10. https://doi.org/10.1155/2018/6852165

Omatsola, M. E., & Adegoke, O. S. (1981). Tectonic evolution and cretaceous stratigraphy of the Dahomey Basin, Nigeria. *Journal of Mining and Geology*, *18*, 130-137.

Pal, D. K., & Tarafdar, J. C. (2009). Analysis of soil for soil survey and mapping. In *Soil Survey Manual*. NBSS&LUP . Eds.: Bhattacharyya, T., Sarkar, Dipak, Pal, D.K.

Prego, R., Belzunce, M. J., Helios-Rybicka, E., & Barciela, M. C. (1999). Cadmium, manganese, nickel and lead contents in surface sediments of the lower Ulla River and its estuary (Northwest Spain). *Bol. Inst. Esp. Oceanogr*, *15*(1-4), 495-500.

Rahaman, K. (2011). In Assessment of heavy metal contamination of sediments of some polluted rivers (Unpublished M.Sc. Thesis, p. 156). Bangladesh University of Engineering and Technology.

Rauret, G., Rubio, R., Lopez-sanchez, J. F., & Casassas, E. (1989). Specific Procedure for Metal Solid Speciation in Heavily Polluted River Sediments. *International Journal of Environmental Analytical Chemistry*, *35*(2), 89-100. https://doi.org/10.1080/03067318908028382

Ritchie, J. M., Cresser, M., & Cotter-Howells, J. (2001). Toxicological response of a bioluminescent microbial assay to Zn, Pb and Cd in an artificial soil solution: Relationship with total metal concentrations and free ion activities. *Environmental Pollution*, *114*, 129-136. https://doi.org/10.1016/S0269-7491(00)00196-2

Sadhana, P. (2014). Distribution and fractionation of heavy metals in sediments of Karra River, Hetauda, Nepal. *Technology*, *19*(2), 123-128. https://doi.org/10.3126/jist.v19i2.13865

Salomon, W., & Förstner, U. (1984). *Metals in the hydrocycle* (p. 349). Springer-Verlag, New-York Berlin Heidelberg. https://doi.org/10.1007/978-3-642-69325-0

Samuel, A.O., & Olabode, O. S. (2021). Sequential extraction and geochemistry of heavy metals in Ayetoro Coastal sediments, Southwestern Nigeria. *Journal of Ecology and Natural Resources, 5*(4), 1-26. https://doi.org/10.23880/jenr-16000261

Singh, A. K., Hasnain, S. I., & Banerjee, D. K. (1999). Grain size geochemical partitioning of heavy metals in sediments of the Damodar River-a tributary of the lower Ganga, India. *Environmental Geology*, *39*(1), 90-98. https://doi.org/10.1007/s002540050439

Tessier, A., Campbell, P. G. C., & Bisson, M. (1982). Particulate trace metal speciation in stream sediments and relationships with grain size: implications for geochemical exploration. *Journal of Geochemical Exploration*, *16*, 77-104. https://doi.org/10.1016/0375-6742(82)90022-X

Tessier, A., Campbell, P. G. C., & Bisson, M. (1979). Sequential extraction procedure for the speciation of particulate trace metals. *Analytical Chemistry*, 844-851. https://doi.org/10.1021/ac50043a017

Ward, J. H., Jr. (1963). Hierachical grouping to optimize an objective function. *Journal of American Statistician Association*, *58*, 236-244. https://doi.org/10.1080/01621459.1963.10500845

Watts, D. W., & Johnson, M. H. (2012). Geochemical mapping using stream sediments in west central Nigeria. Implications for environmental studies and mineral exploration in West Africa. *Applied Geochemistry*, *27*(6), 1035-1062. https://doi.org/10.1016/j.apgeochem.2012.02.023

Zhao, Z., Zhao, B, Wu, D., Wang, J., & Teng, W. (2022). Distribution and fractionation of potentially toxic metals under different land use patterns in Sub-urban areas. *Polish Journal of Environmental Studies*, *32*(1), 475-483. https://doi.org/10.15244/pjoes/139305